

Supporting Information

A “turn-on” fluorescence sensing for sensitively detecting Cr(VI) via a guest exchange process in Cu NCs@MIL-101 composites

Huijing Chen^a, Bo Peng^a, Ping Zhang^a, Ying Yang^a, Xue Hu^{a*}

^a Anhui Provincial Key Laboratory of Environmental Pollution Control and Resource Reuse; School of Environment and Energy Engineering, Anhui Jianzhu University, Hefei 230601, China.

*Corresponding authors. Tel./Fax: +86-18716318049 (X. Hu).

E-mail addresses: huxue602@163.com (X. Hu)

Table S1 Comparison of fluorescent methods for the detection of Cr(VI) in terms of linear range and the limit of detection (LOD).

System	Mode	Linear range (μM)	Detection limits (μM)	Ref.
GSH-Au NCs	Turn-off	0.017-1.7	0.0017	[1]
Lys/BSA-Ag/AuNCs	Turn-off	0.003-0.11	0.00037	[2]
Cys-Cu NCs	Turn-off	0.2-60	0.065	[3]
11-MUA-AuNCs	Turn-off	-	-	[4]
GSH@CDs-Cu NCs	Ratiometric fluorescent	2-40	0.9	[5]
Cysteamine-Au/Cu NCs	Turn-off	0.2-100	0.08	[6]
Thiosalicylic acid/Cysteamine-Cu NCs	Turn-off	0.1-1000	0.03	[7]
Cu NCs@TA	Turn-off	0.03-60	0.005	[8]
TSA/BSA-Cu NCs	Turn-off	0.05-0.4	0.0035	[9]
Au NCs-CDs	Turn-off	0-10	0.005	[10]
Cu NCs@MIL-101	Turn-on	0.05-1 μM and 1-20 μM	0.05	This work

Table S2 The content of Cu in Cu NCs@MIL-101 before and after reaction with Cr(VI).

Material	Weight percentage	Atomic percentage
Cu NCs@MIL-101 before reaction with Cr(VI)	0.09	0.02
Cu NCs@MIL-101 after reaction with Cr(VI)	0.00	0.00

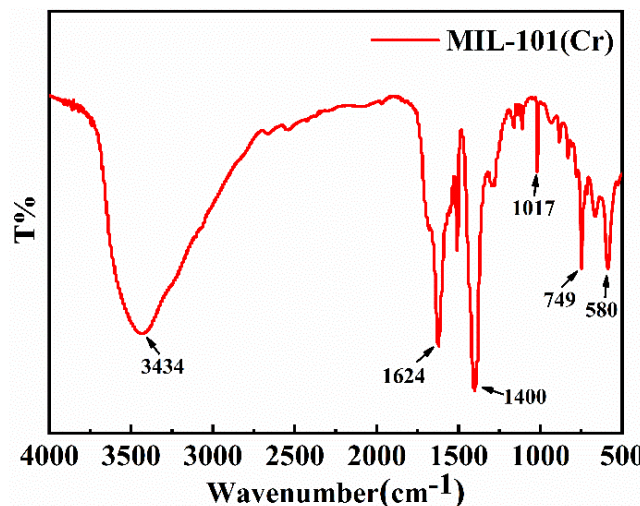


Fig S1 FT-IR spectra of the MIL-101(Cr).

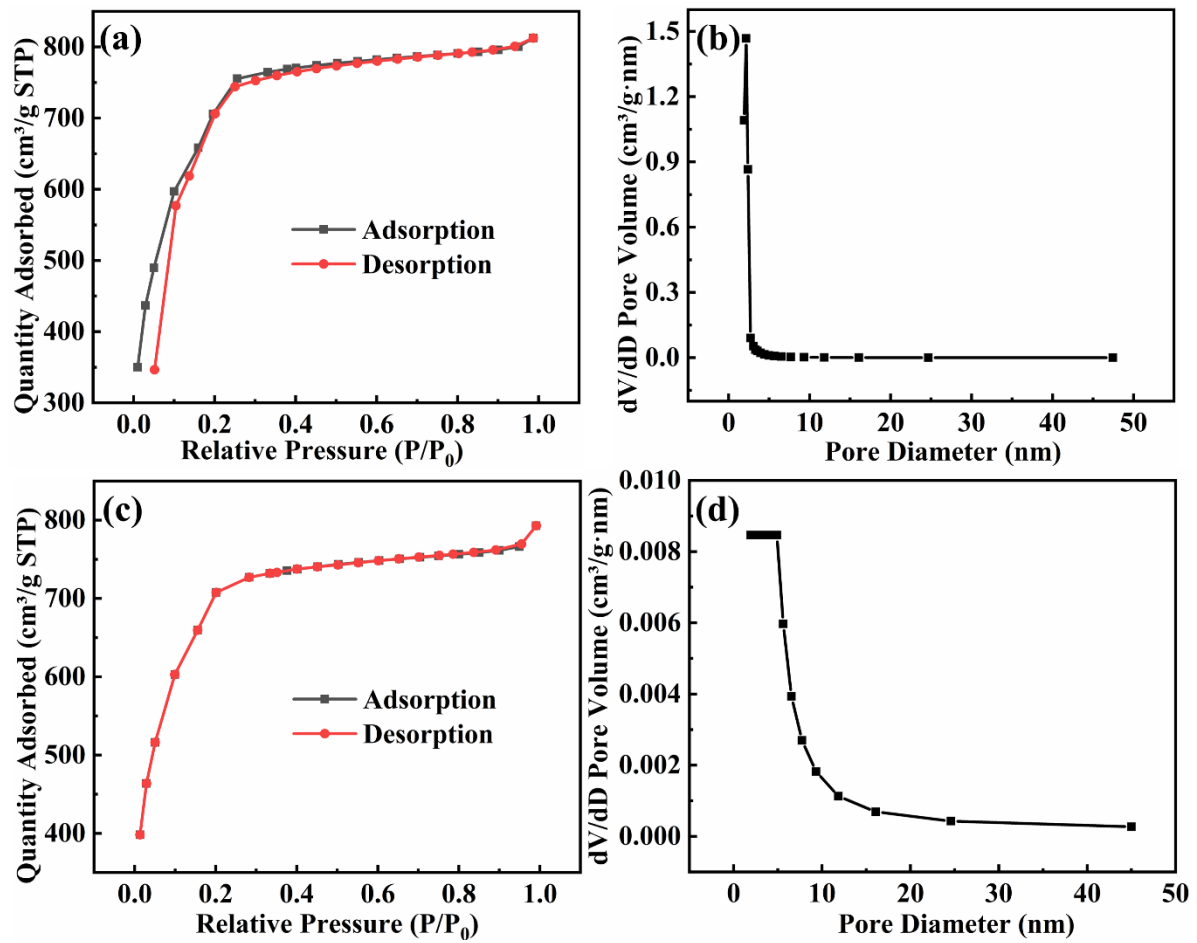


Fig.S2. N₂ adsorption/desorption isotherm of MIL-101(Cr) (a) and Cu NCs@MIL-101 (c), Pore size distributions of MIL-101(Cr) (c) and Cu NCs@MIL-101 (d).

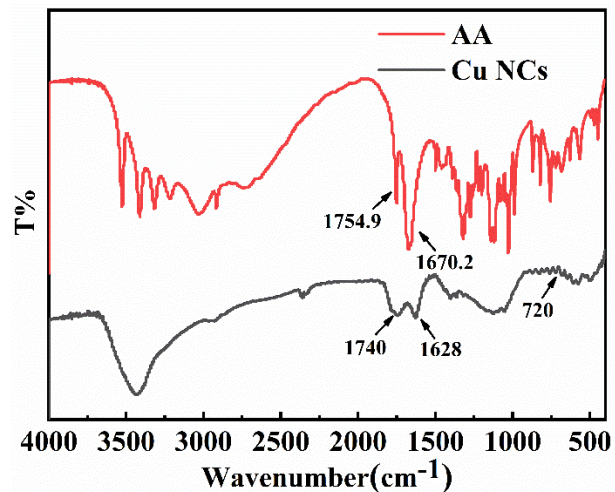


Fig. S3. FT-IR spectra of the AA and Cu NCs.

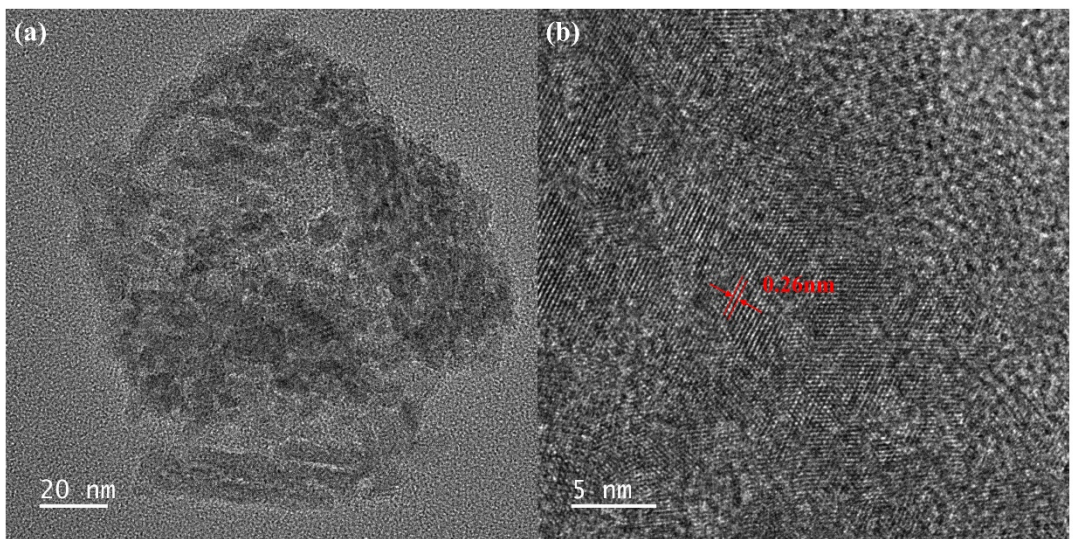


Fig. S4.TEM image (a) and HRTEM image (b) of the Cu NCs.

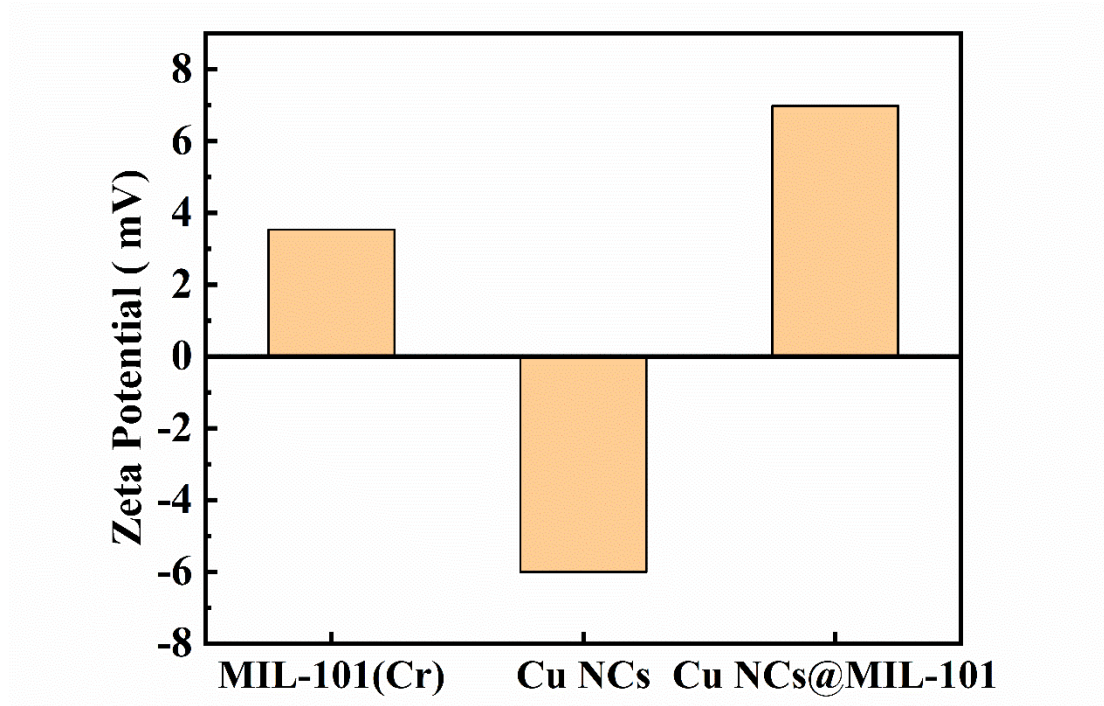


Fig.S5 The zeta potential of MIL-101(VI), Cu NCs and Cu NCs@MIL-101.

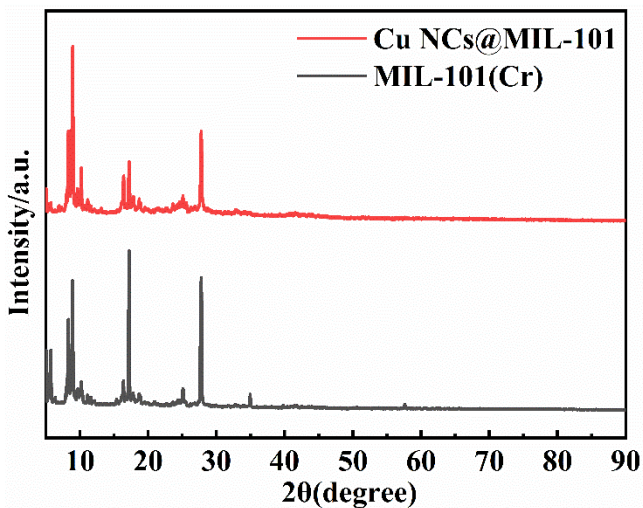


Fig S6 The XRD patterns of the Cu NCs@MIL-101 and MIL-101(Cr).

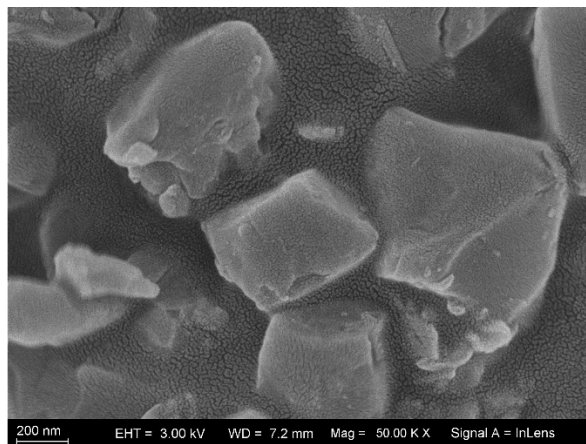


Fig S7 SEM image of Cu NCs@MIL-101.

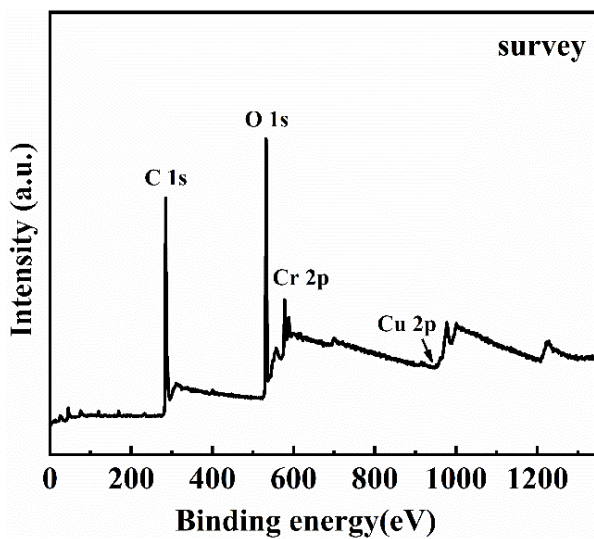


Fig S8 The XPS survey spectrum of the prepared Cu NCs@MIL-101(Cr).

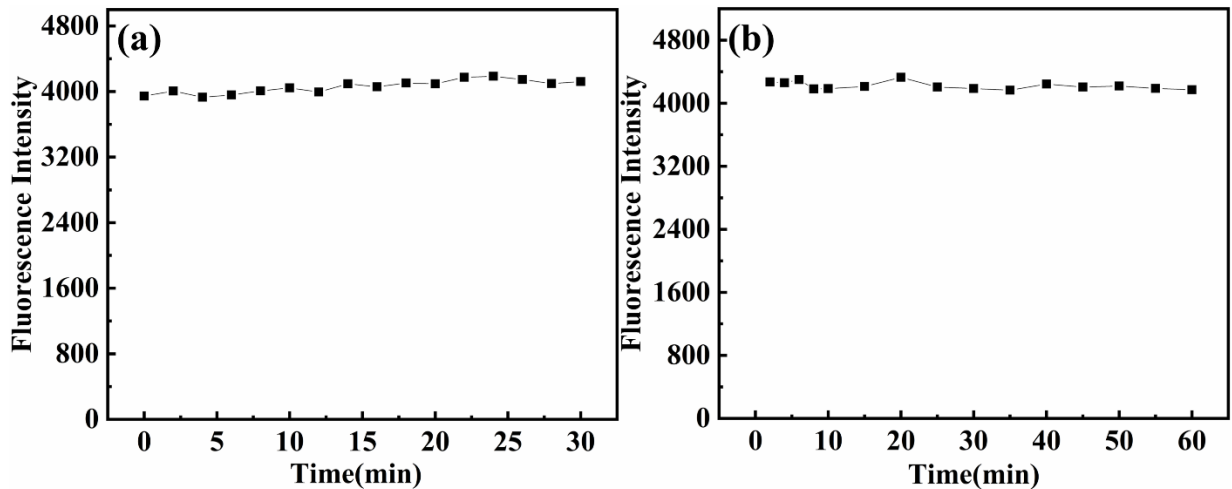


Fig.S9 (a) Photostability of the Cu NCs@MIL-101. Irradiation source: 150 W Xe lamp. (b) Variation of fluorescence intensity of Cu NCs@MIL-101 with time

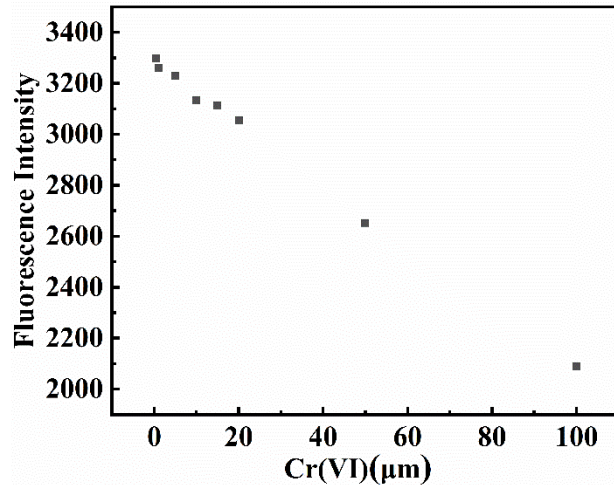


Fig S10 The Fluorescence response of Cu NCs alone interact with Cr(VI).

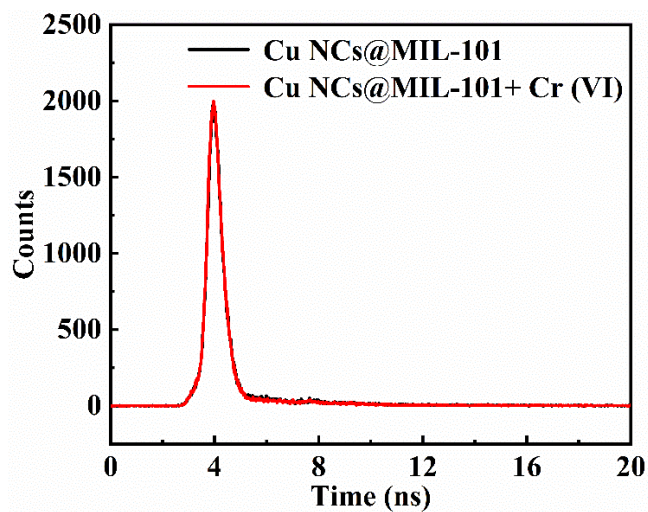


Fig S11 The fluorescence lifetime decay curves of Cu NCs@MIL-101 with and without Cr(VI).

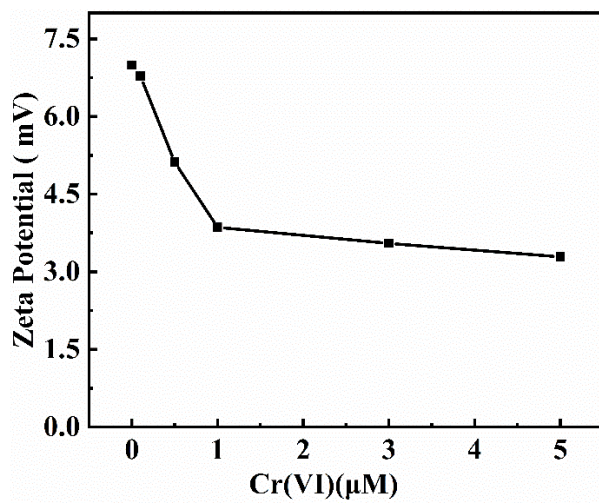


Fig.S12 The zeta potential of Cu NCs@MIL-101 under different concentrations of Cr(VI) ranging from 0.0 to 5.0.

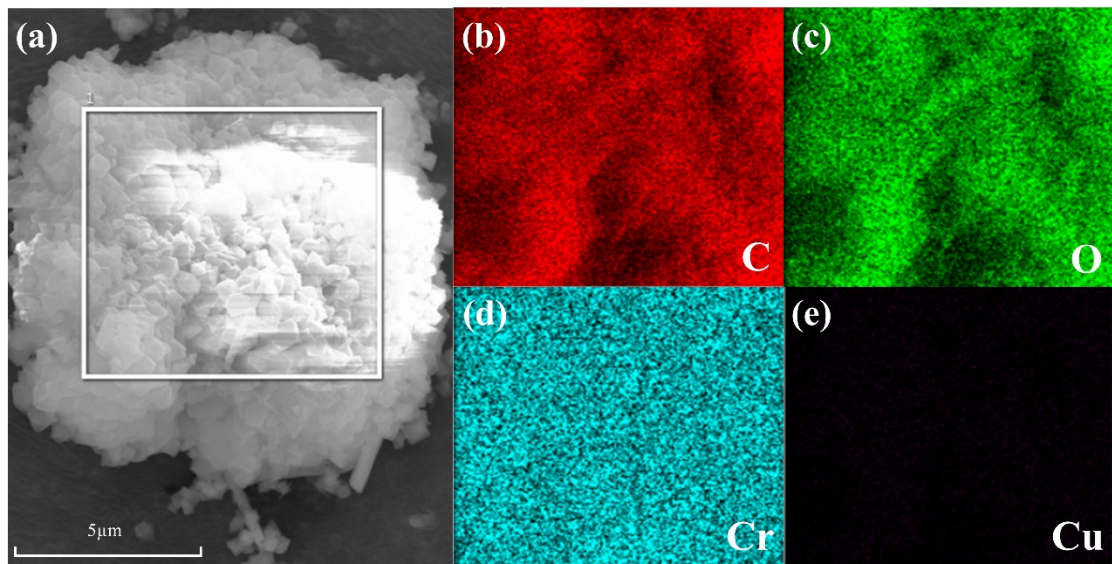


Fig S13 (a) SEM images of Cu NCs@MIL-101. (b-e) EDS images of C, O, Cr and Cu elements in Cu NCs@MIL-101 after reaction with Cr(VI).

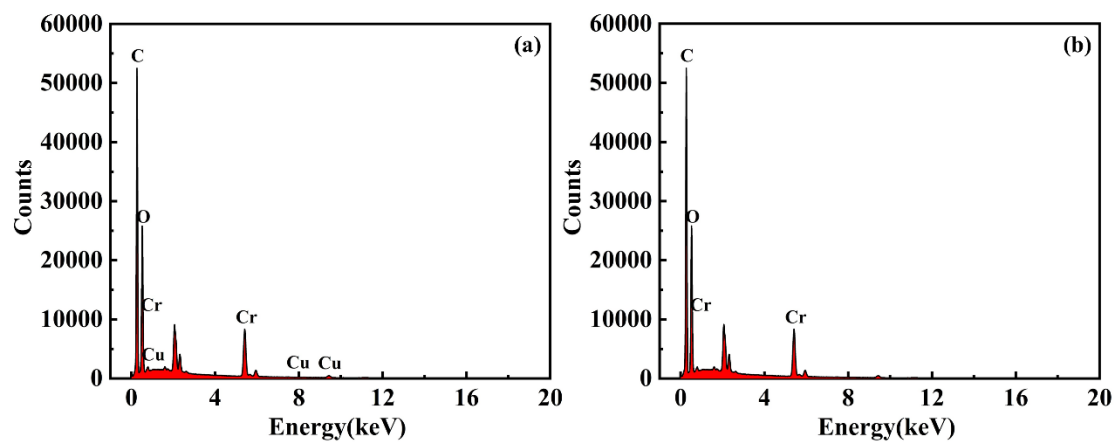


Fig. S14 SEM-EDS analysis result of Cu NCs@MIL-101 (a) and after reaction with Cr(VI) (b).

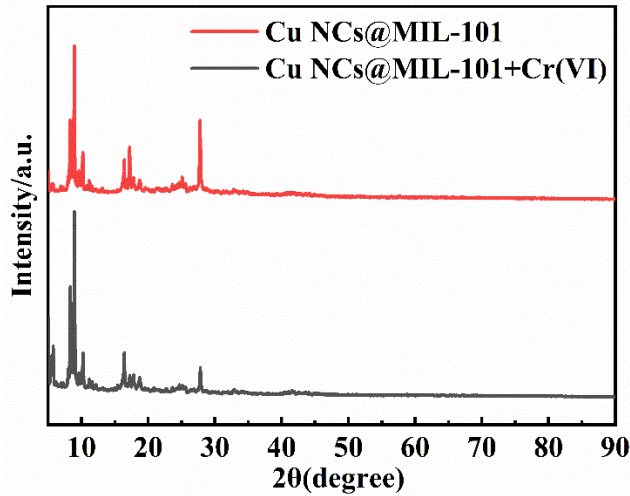


Fig S15 The XRD patterns of the Cu NCs@MIL-101 with and without Cr(VI).

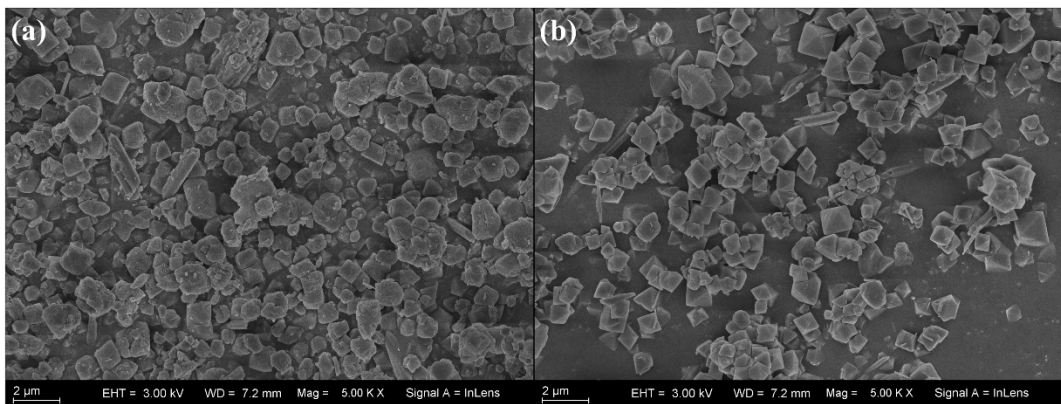


Fig S16 SEM image of Cu NCs@MIL-101 before (a) and after (b) reaction with Cr(VI).

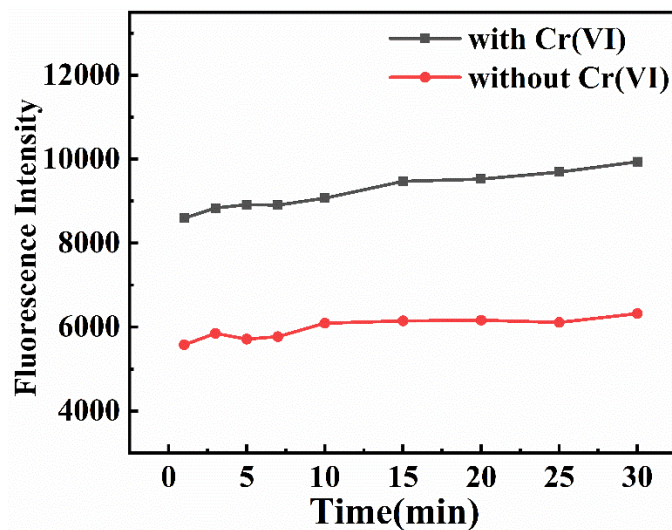


Fig S17 The reaction kinetic between the Cu NCs@MIL-101 pair and Cr(VI).

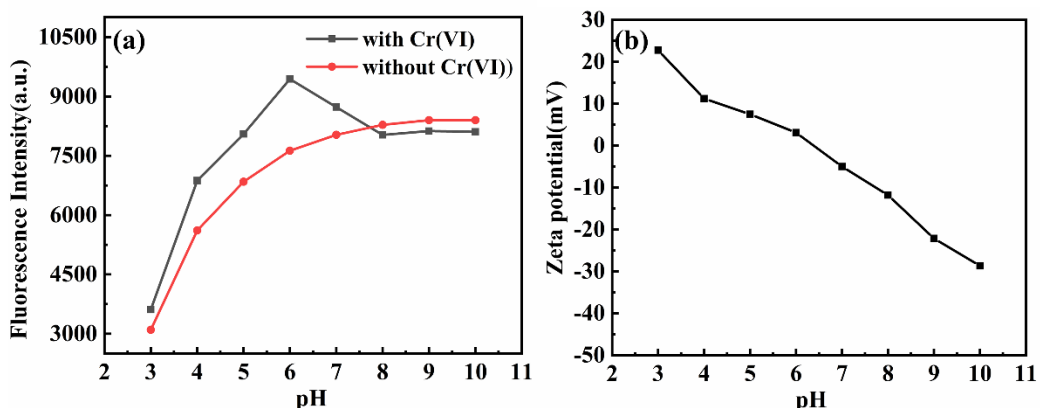


Fig S18 The influence for the fluorescence response of Cr(VI) for the Cu NCs@MIL-101 pair from pH change (a) and the zeta potential of Cu NCs@MIL-101 under different solution pH ranging from 3.0 to 10.0 (b).

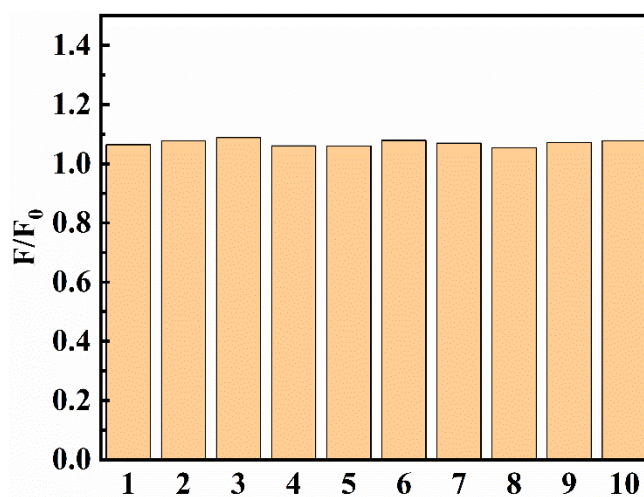


Fig S19 Ten parallel samples of Cu NCs@MIL-101 reacted with Cr(VI) ($10\mu\text{M}$).

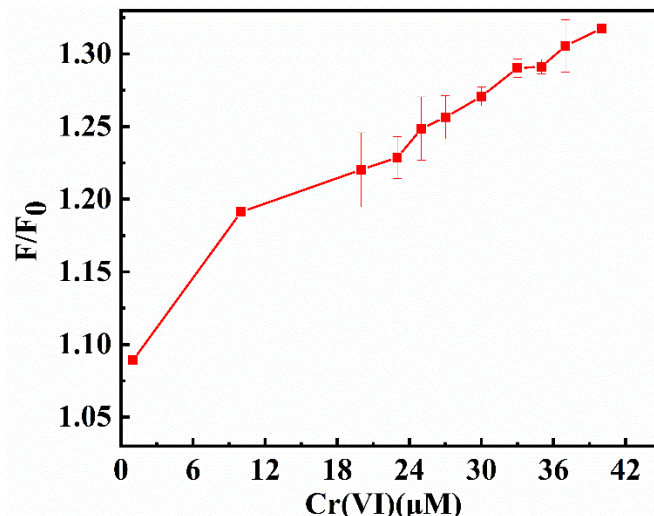


Fig S20 The variation of fluorescence intensity of the Cu NCs@MIL-101 pair with the amounts increasing of Cr(VI) from 0 to $40\mu\text{M}$.

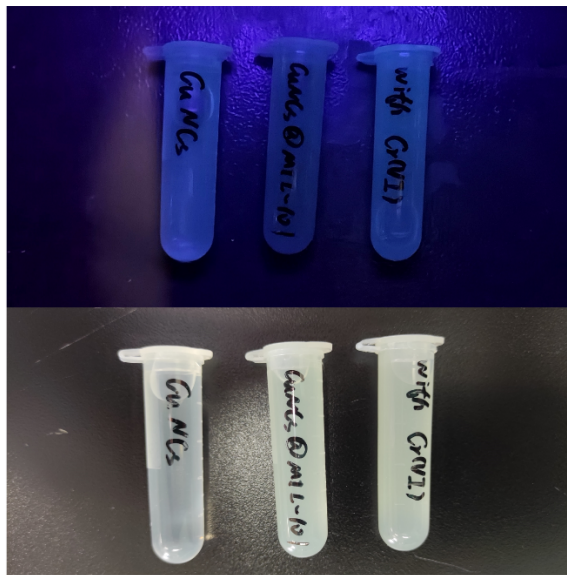


Fig.S21 Naked eye observation of Cu NCs (left), Cu NCs@MIL-101 before (middle) and after reaction with Cr(VI) (right) under UV light (above) and sun light (under).

References

1. H. Y. Zhang, Q. Liu, T. Wang, Z. J. Yun, G. L. Li, J. Y. Liu, and G. B. Jiang, *Anal Chim Acta.*, 2013, 770, 140-146.
2. Z. J. Cheng, Y. C. Fan, L. Zhang, and C. Wang, *J Mol Struct.*, 2023, 1275, 134712.
3. M. L. Cui, G. Song, C. Wang, and Q. J. Song, *Microchim Acta.*, 2015, 182, 1371-1377.
4. J. Sun, J. Zhang, and Y. D. Jin, *J Mater Chem C.*, 2013, 1, 138-143.
5. H. Y. Bai, Z. Q. Tu, Y. T. Liu, Q. X. Tai, Z. K. Guo, and S. U. Liu, *J Hazard Mater.*, 2020, 386, 121654.
6. M. Shellaiah, T. Simon, N. Thirumalaivasan, K. W. Sun, F. H. Ko, and S. P. Wu, *Microchim Acta.*, 2019, 186, 1-8.
7. Y. S. Lin, T. C. Chiu, and C. C. Hu, *RSC Adv.*, 2019, 9, 9228-9234.
8. X. L. Cao, Y. G. Bai, F. X. Liu, F. Li, and Y. N. Luo, *Luminescence.*, 2021, 36, 229-236.
9. A. Nain, Y. T. Tseng, Y. S. Lin, S. C. Wei, R. P. Mandal, B. Unnikrishnan, C. C. Huang, F. G. Tseng, and H. T. Chang, *Sensor Actuat B-Chem.*, 2020, 321, 128539.
10. L. Y. Yu, L. Y. Zhang, G. J. Ren, S. Li, B. Y. Zhu, F. Chai, F. Y. Qu, C. G. Wang, and Z. M. Su, *Sensor Actuat B-Chem.*, 2018, 262, 678-686.